BaTiO$_3$ and TeO$_2$ based gyroscopes for guidance systems: FEM analysis

Zafer Ozer, Amirullah M. Mamedov & Ekmel Ozbay

Taylor & Francis
Taylor & Francis Group

BaTiO$_3$ and TeO$_2$ based gyroscopes for guidance systems: FEM analysis

Zafer Ozer[a], Amirullah M. Mamedov[b,c] and Ekmel Ozbay[b]

[a]Mersin University, Mersin, Turkey; [b]Bilkent University, Nanotechnology Research Center (NANOTAM), Ankara, Turkey; [c]International Scientific Center, Baku State University, Baku, Azerbaijan

ABSTRACT

This paper presents the design, modeling and finite element model simulation of a micro-electromechanical system based on the ternary ferroelectric compounds and paratellurite. The dynamic behavior of the sensor structure is described by the super position of its dominant vibration mode shapes. The resulting model still considers all the physical domains and is even able to capture nonlinear phenomena, such as the stress stiffening of constraint structures or frequency and stiffening caused by squeezed gas in the sensor cell. Process induced and thermally induced residual stresses and the resulting deformation of the transducer elements are considered.

1. Introduction

The Coriolis Effect is the main idea of micromachined gyroscopes, in which the rotation rate will cause the Coriolis force to react in a direction perpendicular to the rotation axis. There are many types of micro-electromechanical system (MEMS) gyroscopes that are commercially available now. There are many differences in the individual MEMS devices; most of them are vibratory-type gyroscopes. They include tuning fork vibration structures [6], ring structures [9], rotational mass or gimbal structures [10], parallel vibration mass [11] and so on. Recently, miniaturized gyroscopes have attracted a lot attention because of their several applications such as automobile industry, satellite posture control, consumer electronics, missiles, etc [2–8].

Maenaka (2006) introduced a novel gyroscope that consists of a rectangular prism bulk-PZT (Lead Zirconate Titanate) with some electrodes placed on the surface [1]. This simple and massive structure is the same as acceleration sensors. Because of such gyroscopes, an unwanted movement of the mass, shock or acceleration is caused resulting in the detection error and collisions of mass by electrodes or sensor body, springs failure, in which permanent damage or the prevention of reference vibration will appear. Hence vibratory micromachine gyroscopes could not operate under shock or large accelerations.

In this study, we design novel structures that are sensitive to biaxial angular velocity and are shock resistant. In addition, we discuss the fixing problem of the gyroscope, analyze the

---

CONTACT Zafer Ozer ✉ zaferozer@hotmail.com

Color versions of one or more of the figures in this article can be found online at www.tandfonline.com/gfer.

principle of operation, and find a resonance mode detecting point. Piezoelectric microma-chined gyroscope (PMMG) is completely solid and has a simple structure [17]. When the mode frequency AC voltage is applied, mode vibration of piezoelectric materials obtained (as material we used $BaTiO_3$ and paratellurite as reference vibrations. MEMS devices are based on physical mechanisms which are capacitive, piezoresistive, electromagnetic, piezo-electric, ferroelectric, optical and tunneling. The most successful type is capacitive transduc-tion [12–15].

2. Mems gyroscope structure, design and simulation

ANSYS is a multiphysics finite element analysis (FEA) software package [16]. FEA is a numerical method for the deconstruction of a complex system by very small parts (user-specified size) called elements. A mesh of 3D coupled-field solid element (Solid5 with 8 DOF) is used for analyzing the device within ANSYS. The software creates a comprehensive explanation of how the system acts as a whole by solving all the implemented equations that govern the behavior of these elements.

For $BaTiO_3$, the 16th and 20th mode shapes are in-plane modes that occur at 514 kHz, and 581 kHz, for TeO_2, the 14th, 20th, 23rd and 28th mode shapes are in-plane modes that occur at 194 kHz, 274 kHz, 321 kHz and 357 kHz. The first mode is in the deriving, x-direc-tion, which only affects the middle frame.

For $BaTiO_3$, the 16th mode is in the sensing, x-direction, which exclusively affects the proof mass since it is the only mass that has a DOF in that direction. The 20th mode also vibrates in the driving direction but the middle and outside frames vibrate out of phase with each other.

Maenaka etc., proposed a novel piezoelectric solid gyroscope in 2006 [1], which is called a piezoelectric micromachined modal gyroscope (PMMG) [13]. Figure 1 shows the basic oper-ation principle of the device. Primarily it is assumed to be a rectangular prism made of $BaTiO_3$ and the polarized z axis.

Figure 2 shows the mode shape of the $BaTiO_3$ prism when we excite the high order reso-nance mode where the differential vibration of the mass elements is almost along the x-axis Figure 3(a) At this resonance mode, the device is ready for angular velocity detection. When the angular velocity is applied along the y-axis, the Coriolis force occurs by the movement of a mass element in Figure 3 (b) resulting in tensile and compressive stresses depending on the position. As shown in figure 3 (c), these stresses generate the piezoelectric voltage on the surface of the device differentially. As an output signal of device this voltage is proportional with the applied angular rate. The substrate block is selected as the piezoelectric ceramic material $BaTiO_3$.

In figure 1, D+ and D− are the driving electrodes, R1 and R2 are the reference electrodes that can be used for tracking and searching for the working resonance mode. A, B, C and D are the sensing electrodes. Without any angular input, because of the symmetry of the piezo-electric structure, the voltage of two adjacent electrodes, for example A and B or, C and D, become equal. When an angular rotation is applied in any direction perpendicular to the modal vibration, the voltage of the sensing electrodes is changed the Coriolis effect, and then the voltage of the two adjacent electrodes are not equal. The rotation input can be quantized via detecting the voltage difference of two adjacent sensing electrodes. The sensing and driving electrodes are distributed in the corresponding positions on the bottom surface as on the top
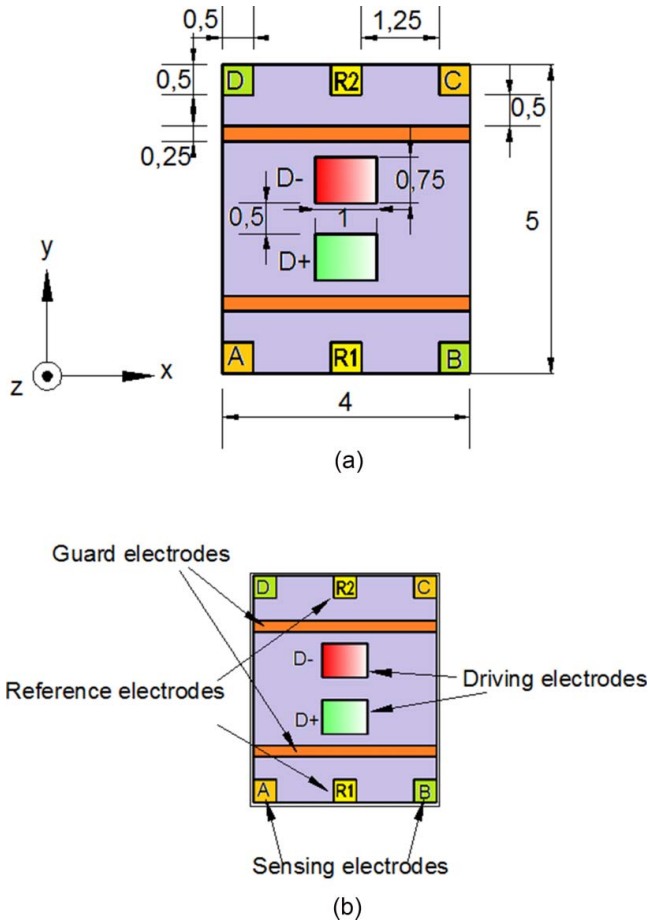
Figure 1. The structure of single-axis PMMG (a) Sizes of PMMG [mm] (b) The layout of electrodes.

surface. The simulation results for paratellurite in the main directions are very close to BaTiO$_3$'s results, but the efficiency of paratellurite based PMMG is lower than the same parameters for BaTiO$_3$. Therefore below we will only discuss BaTiO$_3$'s simulation results hereunder.

3. Result and discussions

A. *Material selection*

As an electro-mechanic transducers, piezoelectric materials are commonly used wherein the requirements for the performance of piezoelectric material vary for different conditions and applications. In this study the piezoelectric material has been used as both the excitation source and the sensing element at same time, and so the piezoelectric material must have larger piezoelectric constant d_{33} and electromechanical coupling constants k_{33} and k_{15}. Based on these conditions, we selected BaTiO$_3$ and TeO$_2$ during the following simulation. Piezoelectric properties of the BaTiO$_3$ and TeO$_2$ obtained from literature [18]. Table 2 shows material parameters of BaTiO$_3$ and TeO$_2$.
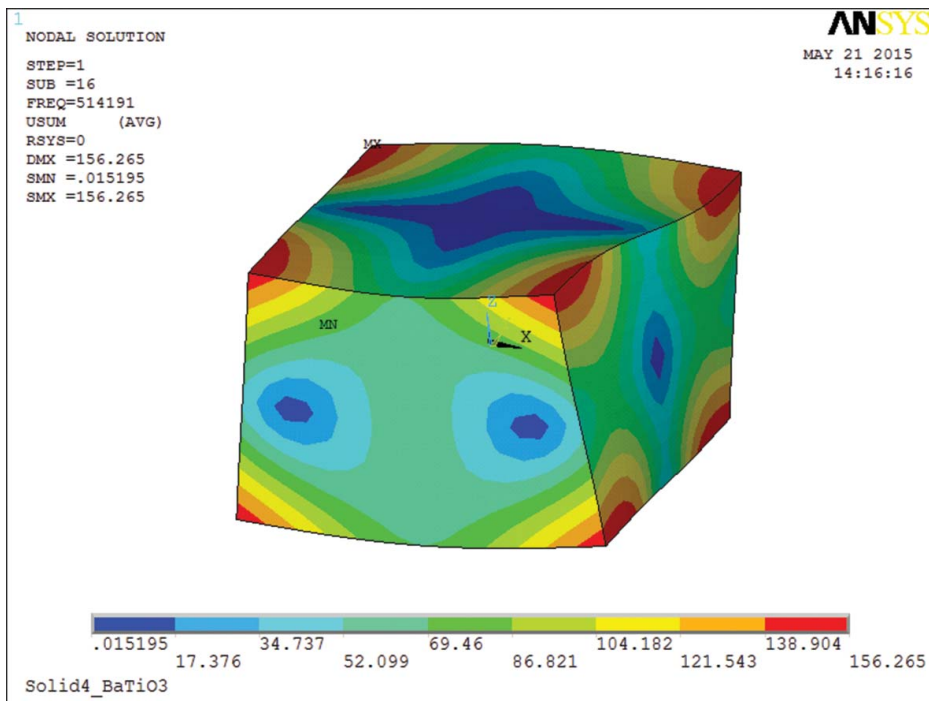
Figure 2. 16th mode. Mass elements almost vibrate parallel to the x-direction.

B. *Modal analysis*

In this section, to find the operation mode the finite element analysis of the piezoelectric body of the PMMG was conducted first. Then to evaluate these modes quantitative indicators were introduced and then best operation mode and the corresponding size of the device were given.

It can be concluded that, from the operation principle, PMMG should have the following characteristics at the working resonance mode.

1. The movement of points in the piezoelectric block should be almost in one direction, x-axis, in this paper.
2. The moving direction of the points should be perpendicular to the polarization direction of the piezoelectric block.
3. The moving direction of a point on one edge is the same as that of the corresponding point on the diagonal edge and is opposite to that of the corresponding point on the adjacent edge.
4. Moving edges should be in a state of tension or compression. To get this special modal shape, we used ANSYS to perform modal analysis and list the corresponding frequencies under which the modal shapes meet these characteristics.

From the numerical study we obtained the following results: Figure 2 shows 16.th mode shape of BaTiO$_3$ PMMG at 514 kHz. It is seen from this figure that maximum stress is occurs at the part of the edges of the PMMG. This shows the location of electrodes placing on surface of the PMMG for the obtaining maximum sensitivity of the sensor. The corresponding results for all BaTiO$_3$ PMMG are listed in Table 1.
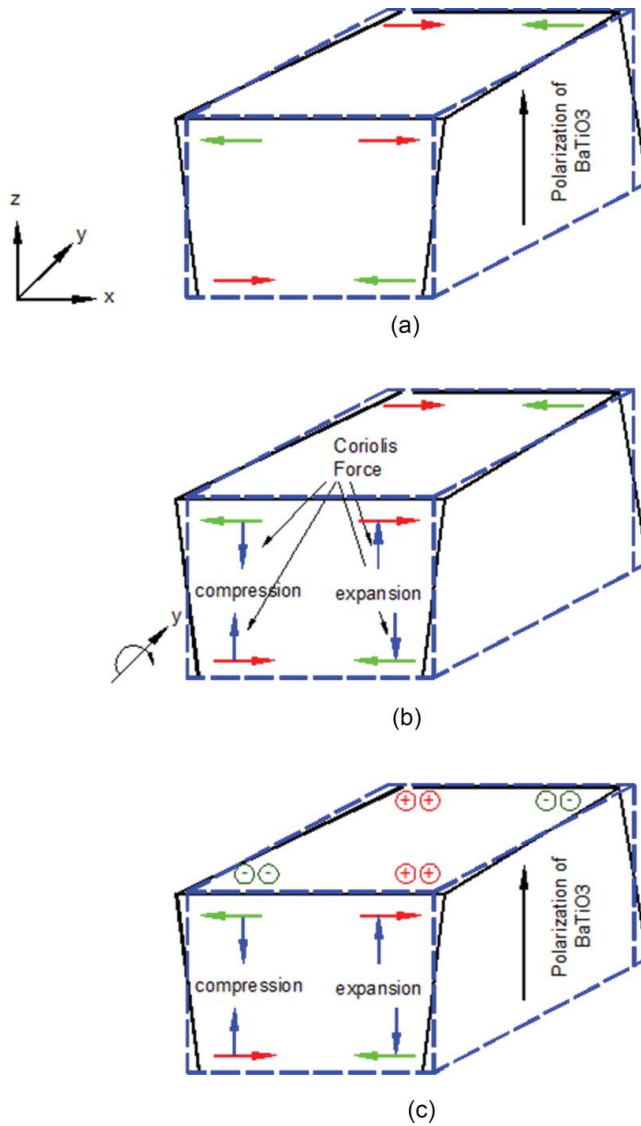
Figure 3. Operation principal of PMMG (a) Reference vibration: BaTiO$_3$ mass element's movement in the x-direction (b) Coriolis Force generated by applied angular rate on moving mass element (c) Compressive/expansive forces induced in surface potential by piezoelectric effect.

**Table 1.** Obtained mode frequencies via modal analysis of BaTiO$_3$ made PMMG.

MODE	1	2	3	4	5	6	7	8	9
BaTiO$_3$	0	0	0	0.0367	0.0419	0.0538	333349	338684	358824
MODE	10	11	12	13	14	15	16	17	18
BaTiO$_3$	410679	444349	446610	467936	475407	509696	514191	517759	519432

Table 2. Material parameters of $BaTiO_3$ and TeO_2.

|	$BaTiO_3$	TeO_2
ε_{11}	2920	22.9
ε_{33}	168	24.7
ρ	6020	5990
e_{31}	-2.69	0
e_{33}	3.65	0
e_{15}	21.3	0
c_{11}	27.5×10^{10}	5.7×10^{10}
c_{12}	17.9×10^{10}	2.24×10^{10}
c_{13}	15.2×10^{10}	5.35×10^{10}
c_{33}	16.5×10^{10}	5.7×10^{10}
c_{44}	5.43×10^{10}	2.65×10^{10}
c_{66}	11.3×10^{10}	6.68×10^{10}

4. Harmonic analysis

A driving voltage should be applied to actuate the device in real applications. To verify the mode shape we excite the 16th mode frequency from the modal analysis, and to perform harmonic analysis we used ANSYS®. The placement of the driving electrodes is shown in figure 1. The driving electrodes D+ and D- excited by 10 Vpp AC voltages with 180° phase difference. The damping constant of the piezoelectric material was assumed as the value of 0.02. The frequency of the driving voltage was scanned 350 kHz to 850 kHz. Figure 5a show the harmonic excitation analysis result in which the x-axis refers to the frequency of the driving voltage and the y-axis refers to the piezoelectric voltage amplitude on the reference
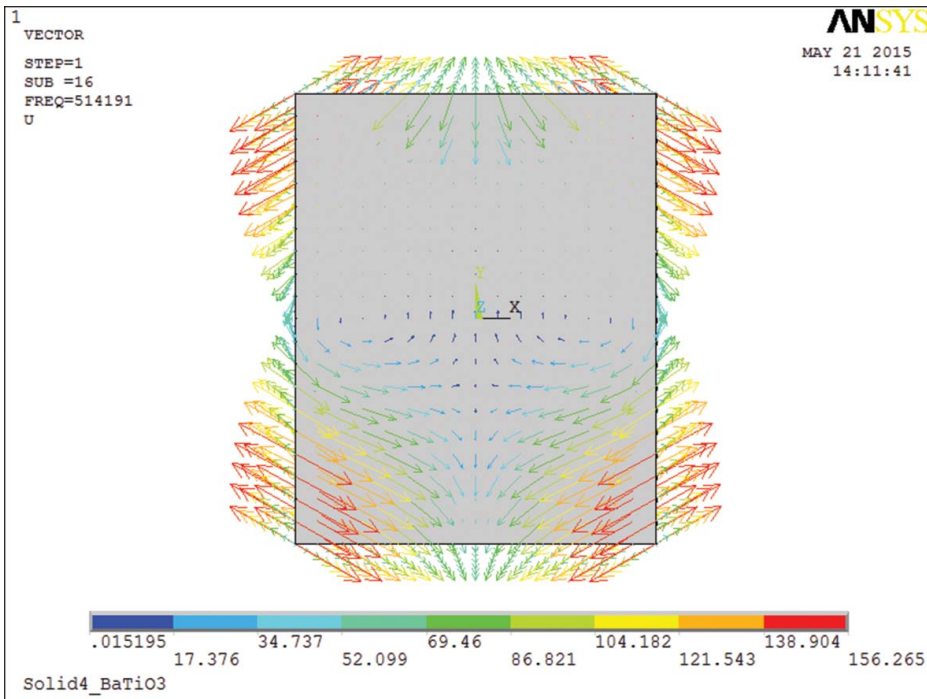
Figure 4. Node displacement vectors on top surface of the 16th mode (514 kHz) for $BaTiO_3$.
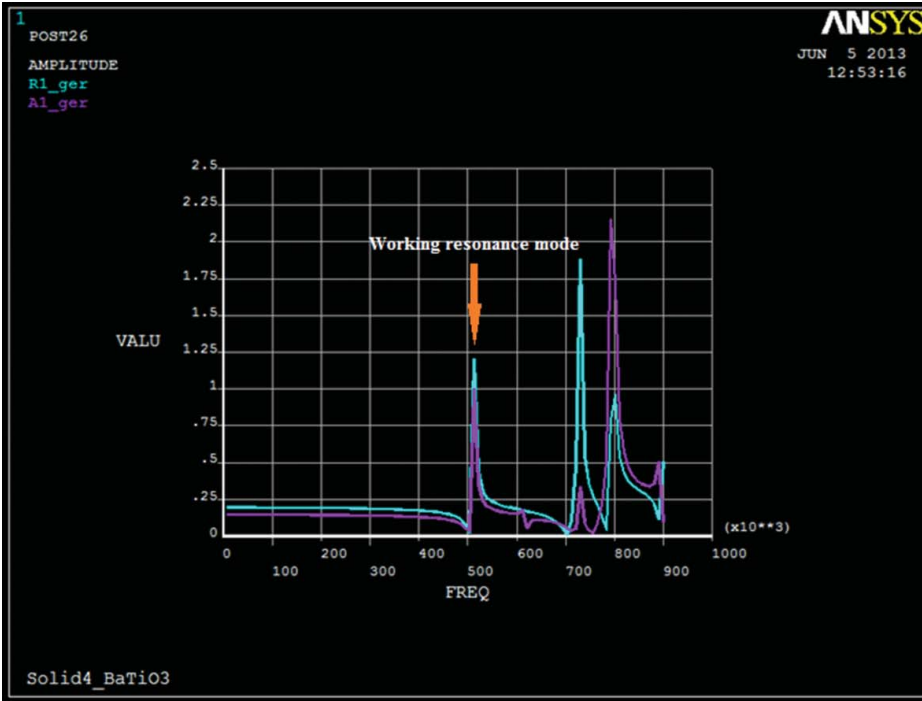
(a)
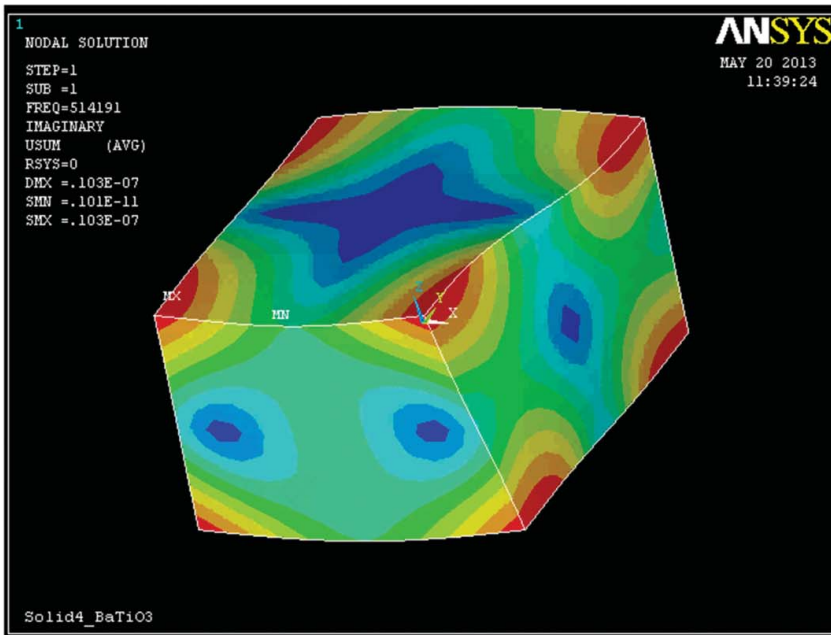
(b)

Figure 5. (a) Harmonic analysis results of the PMMG (frequency of the working resonance mode is 514 kHz) (b) Harmonic excitation analysis result of the BaTiO$_3$ PMMG.
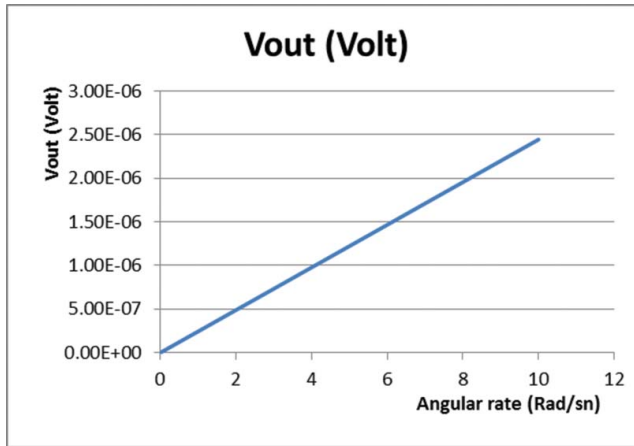
Figure 6. Output voltage vs. applied angular rate for $BaTiO_3$.

electrode, R1 or R2. From the figure, we can see that there are three peaks of the voltage of the reference electrode ($BaTiO_3$). The peak corresponding to the resonance mode is in the position of around 514 kHz. The frequency of the working resonance mode is 514 kHz for $BaTiO_3$.

In addition, from Figure 4 we can observe the node displacement directivity of our model. The figure shows that there is more kinetic energy stored in the effective vibration. Figure 5.b shows the mode shape at the exciting frequency of the working resonance mode for $BaTiO_3$. It is observed that the exciting vibration of the piezoelectric block is the same as the vibrating shape of the working resonance mode.

When we applied the working resonance mode frequency driving voltage to the driving electrodes, the vibration of the working resonance mode can be the actuated account of the Coriolis force. The reason for the raw result of the output voltage for the applied angular velocity is differential with respect to $x = 0$, we implemented the subtraction of the potentials at symmetric points, that is, $Vsub_1 = VB - VA$ and $Vsub_2 = VC - VD$. Figure 6 gives the relation between the angular velocity applied to device and the $Vsub1+Vsub2$.

It is clear that, in Figure 6, $Vsub1+Vsub2$ have a liner relation with angular velocity, which agrees with the working principle of PMMG and verify that the rotation input can be quantized by detecting the voltage difference of two adjacent sensing electrodes. In order to optimize the size of the additional driving electrodes, we introduced three variables that should be changed: the length of the driving electrodes, the voltage applied on the driving electrodes, and the distance between two adjacent electrodes.

5. Conclusion

In this paper, to determine the best operation mode of PMMG modal analysis we first developed a set of quantitative indicators to evaluate the various operation modes.

For heavy acceleration and shock environment, the longitudinal vibrating gyroscope presented here will be one of the candidates for the next generation of gyroscopes. Furthermore, according to the analysis result, it is concluded that the model with integrated masses has a better vibration quality of the resonance mode and higher sensitivity to the rotation.

Acknowledgments

References

[1] K. Maenaka and H. Kohara, Novel solid micro-gyroscope. In: *Proceedings of micro electro mechanical systems workshop MEMS 2006*, Istanbul, Turkey., pp 634–639 (2006).

[2] H. Xie and G. K. Fedder, Integrated microelectromechanical gyroscopes. *J. Aerosp. Engrg.*, **16**, 65–75 (2003).

[3] Y. Chen, J. Jiao, B. Xiong, L. Che, X. Li, and Y. Wang, A novel tuning fork gyroscope with high Q-factors working at atmospheric pressure. *Microsyst. Technol.* **11**, 111–116. doi:10.1007/s00542-004-0438-8, (2005).

[4] B. Zhang, Overview and improving fiber optic gyroscope based on MEMS/NEMS fabrication. *J. Phys. Conf. Ser.*, **34**, 148–154 (2006).

[5] Y. Kagawa, N. Wakatsuki, T. Tsuchiya, and Y. Terada, A tubular piezoelectric vibrator gyroscope. *J. IEEE Sensors* **6**(2), 325–330 (2006).

[6] F. Duan, J. Jiao, Y. Wang, Y. Zhang, B. Mi, J. Li, and Y. Wang, A novel x-axis tuning fork gyroscope with "8 vertical springs-proof mass" structure on (111) silicon. *Microsyst. Technol.* **14**, 1009–1013. doi:10.1007/s00542-007-0527-6 (2008).

[7] Y. Xu, R. Wang, S. K. Durgam, Z. Hao, and L. Vahala, Numerical models and experimental investigation of energy loss mechanisms in SOI-based tuning-fork gyroscopes, *Sens. Actuators A* **152**, 63–74 (2009).

[8] N. C. Tsai, W. M. Huang, and C. W. Chiang, Magnetic actuator design for single-axis micro-gyroscopes. *Microsyst. Technol.*, **15**, 493–503. doi:10.1007/s00542-008-0769-y, (2009).

[9] F. Ayazi and K. Najafi, A HARPSS Polysilicon Vibrating Ring Gyroscope, *J. Microelectromech. Syst.* **10**, 169–179 (2001).

[10] T. Fujita, K. Hatano, K. Maenaka, T. Mizuno, T. Matsuoka, T. Kojima, T. Oshima, and M. Maeda, Vacuum Sealed Silicon Bulk Micromachined Gyroscope, in Digest Tech. Papers Transducers '99 Conference, Sendai, pp. 914–917, (1999).

[11] K. Maenaka, T. Fujita, Y. Konishi, and M. Maeda, Analysis of a high sensitive silicon gyroscope with cantilever beam as vibrating mass, *Sensors Actuators* **A54**, 568–573 (1996).

[12] D. H. Li, X. J. Zheng, B. Wu, and Y. C. Zhou, Fracture analysis of a surface through-thickness crack in PZT thin film under a continuous laser irradiation. *Eng. Fract. Mech.* **76**, 525–532 (2009).

[13] X. Wu, W. Chen, W. Zhang, Y. Lu, F. Cui, and X. Zhao, Modeling Analysis of Piezoelectric Micromachined Modal Gyroscope. In: Proc. Of the IEEE Intern. Conf. on Nano-Micro Engineered and Molecular Systems, Shenzhen, China (2009).

[14] Y. Lu, X. Wu, W. Zhang, W. Chen, F. Cui, and W. Liu, Optimization and analysis of novel piezoelectric solid micro-gyroscope with high resistance to shock, *Microsyst. Technol.*, **16**, 571–584 (2010).

[15] Y. Lu, X. Wu, W. Zhang, W. Chen, F. Cui, and W. Liu, Optimal special vibration used as reference vibration of vibratory gyroscopes, *Electron. Lett.*, **46**(2) (2010).

[16] www.ansys.com

[17] X. Hu, X. Wu, Z. Wang, W. Chen, and W. Zhang, Model Design of Piezoelectric Micromachined Modal Gyroscope, *J. Sensors*, ID 106482, (2011).

[18.] www.efunda.com